



ELSEVIER

Journal of Crystal Growth 166 (1996) 375–379

JOURNAL OF **CRYSTAL
GROWTH**

Growth and characterization of $\text{BaLiF}_3:\text{TM}$ (Ni^{2+} , Co^{2+}) for laser applications

S.L. Baldochi^{*}, A.M.E. Santo, E. Martins, M. Duarte, M.M.F. Vieira, N.D. Vieira Jr.,
S.P. Morato

Instituto de Pesquisas Energéticas e Nucleares – IPEN – CNEN / SP, Caixa Postal 11049, São Paulo, SP, Brazil

Abstract

Single crystals of BaLiF_3 doped with different concentrations of Ni^{2+} and Co^{2+} and exhibiting good optical quality were grown from the melt using the Czochralski technique. The preparation and growth conditions are reported. Spectroscopic characterization of these materials indicates that this matrix doped with Ni^{2+} or Co^{2+} is a promising laser-active medium in the spectral region of 1.5 μm .

1. Introduction

BaLiF_3 is an inverse perovskite material with a cubic structure where Ni^{2+} and Co^{2+} impurity ions can occupy octahedral sites. Transition-metal ions in this symmetry give rise to broad-band emissions that are potentially useful as vibronic laser materials [1]. To investigate the optical properties and laser capabilities of these systems, good-quality single crystals with appropriate Ni^{2+} and Co^{2+} concentrations are required. The growth of pure BaLiF_3 crystals with high quality has recently been reported [2,3]. The growth of small Co^{2+} -doped samples has been achieved previously by means of the Bridgman or Czochralski techniques [4]. However, a more-detailed study of the preparation and growth of $\text{BaLiF}_3:\text{Ni}^{2+}$ and $\text{BaLiF}_3:\text{Co}^{2+}$ with different dopant compositions, as well as a complete spectroscopic characterization of these impurities in this matrix has not previously been performed.

In this paper, we report the experimental conditions for growing high-quality Ni^{2+} - and Co^{2+} -doped BaLiF_3 crystals with dopant concentrations in the range of 0.05 to 2.5 mol%. Crystals as large as 20 mm in diameter and 50 mm in length were grown by the Czochralski technique. The Ni^{2+} and Co^{2+} distributions in these BaLiF_3 crystals were measured, and the optical properties of both $\text{BaLiF}_3:\text{Ni}^{2+}$ and $\text{BaLiF}_3:\text{Co}^{2+}$ are reported.

2. Experimental procedure

The starting materials for crystal growth were prepared by standard hydrofluorination methods [5]. BaF_2 synthesized from BaCO_3 (99.999% Aldrich) and LiF (99.99% Alfa) pre-purified by zone refining were weighed and mixed in a non-stoichiometric composition. BaLiF_3 melts incongruently and must be grown from a melt with excess LiF to avoid “other-phase” precipitation. The most-appropriate composition was determined in zone-refining experi-

^{*} Corresponding author. Fax: +55 11 212 3546.

ments considering the phase diagram of the BaF_2 – LiF system [2]. The following molar ratios of the components were used: BaF_2 (43%): LiF (57%), BaF_2 (44%): LiF (56%), BaF_2 (46%): LiF (54%) and BaF_2 (48%): LiF (52%). The best results were obtained for the (44%):(56%) composition [6]. All zone-refining runs were performed under an HF atmosphere in a platinum chamber using vitreous-carbon crucibles. The basic fluorides used and the final compound were analyzed by atomic-emission spectrography, and no spurious contamination was observed.

The crystals were grown in a vacuum-tight Czochralski system equipped with a graphite heater. The NiF_2 (or CoF_2) and pieces of the zone-refined BaLiF_3 bars, which were placed in a vitreous carbon crucible, were previously treated in vacuum and then melted under an argon atmosphere. Even though careful treatment of the system and purification of the argon gas introduced in the furnace were employed, the formation of a thin film on the melt surface was observed. X-ray diffraction analysis showed that it was metallic nickel (or metallic cobalt). Nevertheless, seeding was possible in most of the runs because this metallic “scum” adhered to the crucible walls. In some of the growth runs, the Ni^0 (or Co^0) adhered to the growing crystal – resulting in superficial defects; however, we have not observed cracking associated with these. To minimize this problem, in the last growth runs of BaLiF_3 : Co^{2+} , a reactive atmosphere (CF_4) was used. The metallic thin-film formation was reduced by 70%.

We have utilized 3, 5, 6.5, 8 and 10 mol% of the dopant in the melt. This resulted in actual dopant



Fig. 1. BaLiF_3 : Ni^{2+} crystal grown from a 5 mol%-doped melt.

concentrations ranging from 0.3 to 2.5 mol% in BaLiF_3 : Ni^{2+} and from 0.05 to 0.7 mol% in BaLiF_3 : Co^{2+} . The dopant concentration incorporated along the growth axis of the crystals (Sec. 3.1), was evaluated by atomic-emission spectrographic analysis and neutron-activation analysis (Table 1). It is interesting to note that it was easier to introduce Ni^{2+} ions than Co^{2+} ions in the BaLiF_3 matrix.

The crystals were grown in the $\langle 111 \rangle$ direction at a pulling rate of 1 mm/h and, in most of the experiments, with a rotation rate of 25 rpm (some runs were conducted with lower rotation rates). The growth was terminated when about 50% of the initial material was pulled from the crucible. This was necessary because of the BaLiF_3 incongruent melting. Boules as large as 20 mm in diameter and 40 to 50 mm in length were obtained (Figs. 1 and 2). The crystals were cooled at a rate of $30^\circ\text{C}/\text{h}$.

Table 1
Dopant concentrations

Crystal	Melt concentration (mol%)	Crystal concentration (mol%)	
		Technique 1 ^a	Technique 2 ^b
BaLiF_3 :Ni	3	0.25	0.35
	5	0.80	1.03
	10	2.30	2.50
BaLiF_3 :Co	3	–	0.05
	5	–	0.44
	6.5	–	0.55
	8	–	0.67

^a Atomic emission spectrographic analysis.

^b Neutron activation analysis.

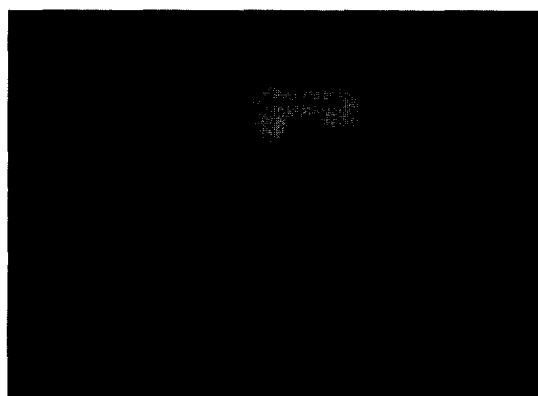


Fig. 2. BaLiF_3 : Co^{2+} crystal grown from a 6.5 mol%-doped melt.

3. Results and discussion

3.1. Impurity distribution

Fig. 3 shows the relative dopant concentration as a function of the fraction of solidified mass in doped BaLiF_3 crystals, where C_s is the concentration of impurity in the solid, C_0 is the initial concentration in the liquid, and g is the solidified fraction. We attempted to fit the measured results to the normal freezing formula [7] ($C_s = kC_0(1-g)^{k-1}$) to estimate the distribution coefficient, k . In two crystals grown with different Ni^{2+} concentrations (3 and 5 mol%), in argon atmosphere, there was no agreement between the experimental and calculated values from the normal freezing formula. This result may possibly be attributed to the metallic thin film observed in all of the growth runs with an argon atmosphere. The above equation holds when the system may be considered close enough to equilibrium, so that $k \approx k_{\text{eff}}$

(effective distribution coefficient). That is, the growth rate is such that the mixing in the liquid is complete, the bulk and the interface-liquid concentration are equal, and the measured k is independent of the stirring speed and growth. A thin film on the melt surface changes the flow near the interface [8] and the stirring conditions resulting in fluctuations in the melt temperature that may cause associated fluctuations of the growth rate. It is also important to note that the Ni^0 formation on the melt surface reduces the bulk Ni^{2+} concentration, modifying the initially measured concentration.

The assumption that the metallic film influences the impurity segregation was confirmed in the $\text{BaLiF}_3:\text{Co}^{2+}$ growth under a CF_4 atmosphere. As already mentioned, the presence of a reactive atmosphere reduced the metallic-film formation by 70%. Fig. 3b shows the experimental and calculated values of the relative concentration along a crystal grown from a 6.5 mol%-doped melt. The agreement between the experimental and the calculated values is rather good; k was estimated to be 0.059 ± 0.002 .

3.2. Optical and crystalline quality

The scattering in a crystal can be qualitatively evaluated by visual observation when a He–Ne laser beam is transmitted through the boule, in the dark. Low-concentration crystals ($C_{\text{melt}} \leq 5$ mol%) showed no scattering. Highly doped crystals have shown scattering in the central regions neighbouring the final part of the boule. This was probably due to LiF and/or TM precipitation in the solid phase. High dopant concentrations change the phase relations and the stoichiometry of the melt, resulting in the segregation of one of the components. Large defects resulting from growth-control instabilities were not observed except for superficial defects resulting from adhesion of the metallic film to the surface of some crystals.

The crystalline quality of the doped crystals was evaluated by neutron diffraction using the same equipment described in Ref. [3] for the study of pure BaLiF_3 crystals. Fig. 4 shows the rocking curves obtained with a pure and a doped sample grown with 5 mol% of NiF_2 in the melt. A fitting done with gaussian curves is also shown in the figure. This fitting allows one to determine the number and char-

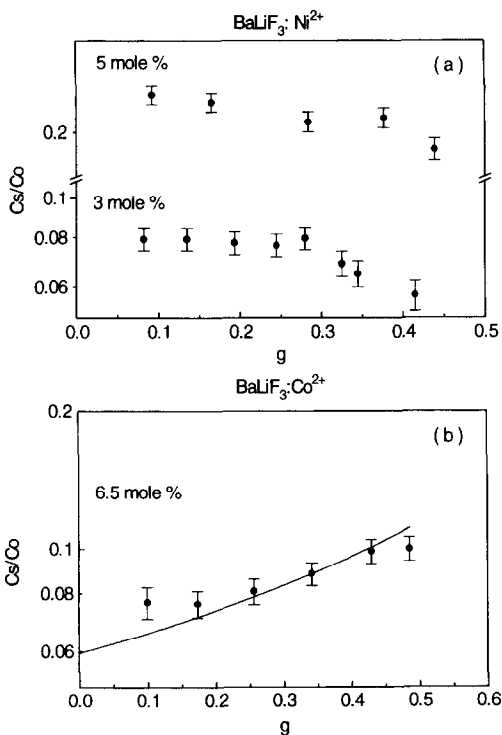


Fig. 3. Impurity distribution of: (a) $\text{BaLiF}_3:\text{Ni}^{2+}$ crystals grown from a 3 and a 5 mol%-doped melt; (b) $\text{BaLiF}_3:\text{Co}^{2+}$ crystal grown from a 6.5 mol%-doped melt.

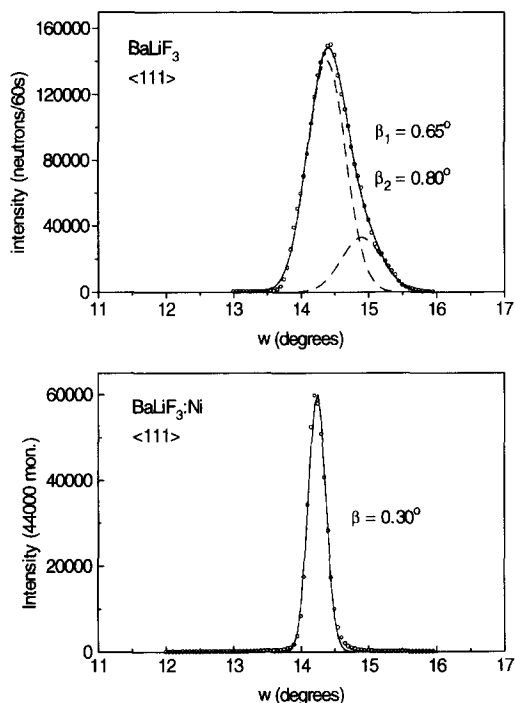


Fig. 4. Rocking curves in the growth direction of a pure (a) and a Ni^{2+} -doped BaLiF_3 crystal (b).

acteristics of the mosaic domains in the crystals. The pure sample has two mosaic blocks approximately 0.5° apart. The larger domain in this sample has a half width (β) of 0.65° and the smaller one of 0.80° . The nickel-doped sample has only one mosaic block with a half width of 0.3° . The differences observed between the two samples are possibly intrinsic to the crystals. Two crystals obtained under similar conditions will not have exactly the same quality [3]. However, we can conclude that the impurity introduction has not lowered the crystalline quality of the BaLiF_3 crystals.

3.3. Optical properties

3.3.1. $\text{BaLiF}_3:\text{Ni}^{2+}$

The basic optical spectroscopic properties of Ni^{2+} in BaLiF_3 were previously studied [9]. The room-temperature absorption spectrum of $\text{BaLiF}_3:\text{Ni}^{2+}$ shows three main broad bands peaking at 1180, 700 and 390 nm. Three bands are observed in the luminescence spectra: the infrared emission, an intense broad band peaking at $1.5 \mu\text{m}$, a red emission at 740

nm and the green emission peaking at 480 nm. The luminescence decay time obtained at room temperature is 2.5 ms, and at 77 K, 5 ms. The emission cross section is $3 \times 10^{-21} \text{ cm}^2$ at the peak of the $1.5 \mu\text{m}$ band. Concerning the topic of practical laser development, this small value of the emission cross section requires crystals with high concentrations. However, in recent studies [10], a concentration-quenching effect was observed in $\text{BaLiF}_3:\text{Ni}^{2+}$ which reduces the luminescence decay time and limits the maximum ideal concentration to 1 mol%. This means that long $\text{BaLiF}_3:\text{Ni}^{2+}$ samples will be necessary ($\sim 2 \text{ cm}$) to obtain initial laser operation.

3.3.2. $\text{BaLiF}_3:\text{Co}^{2+}$

The optical properties presented by the $\text{BaLiF}_3:\text{Co}^{2+}$ crystals are typical of the Co^{2+} ion in pure octahedral symmetry. Two intense absorption bands were observed [11] (Fig. 5): one peaking at 500 nm, and other peaking at 1210 nm, with bandwidths around 20%. Also observed was a weaker band at 600 nm. $\text{BaLiF}_3:\text{Co}^{2+}$ presents only one emission at $1.6 \mu\text{m}$ (1588 nm), with 426 nm of spectral width (FWHM) at room temperature. The luminescent decay time observed at low temperature is 600 μs , lowering to 1.0 μs at room temperature due to multiphonons originated nonradiative transitions which show a strong temperature dependence. The emission cross section is $1.7 \times 10^{-20} \text{ cm}^2$ at the peak of the band. Considering the above optical parameters, the first calculations for laser tests indicate that laser operation in $\text{BaLiF}_3:\text{Co}^{2+}$ crystals will be possible only at liquid nitrogen temperature.

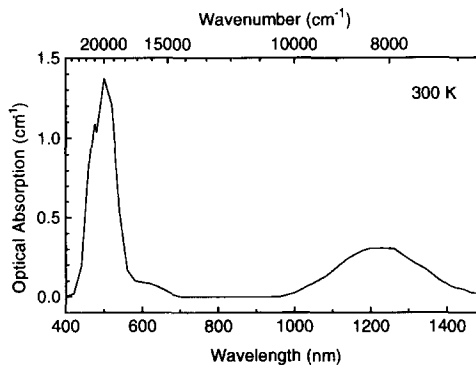


Fig. 5. Absorption spectrum of a $\text{BaLiF}_3:\text{Co}^{2+}$ crystal at room temperature.

4. Conclusions

Good-quality $\text{BaLiF}_3:\text{Ni}^{2+}$ and $\text{BaLiF}_3:\text{Co}^{2+}$ crystals have been grown by the Czochralski technique. Growth under an argon atmosphere always resulted in the formation of a thin metallic film on the melt surface which disturbed the impurity-distribution process in the crystal. Growth under a CF_4 atmosphere reduced by 70% the metallic-film formation, thereby minimizing the problem. The incorporation of Ni^{2+} and Co^{2+} ions in the BaLiF_3 crystals does not change their crystalline quality. Growth with low concentrations (up to 5 mol% in the melt) presented no difficulties regarding possible stoichiometry deviations and/or diffuse scattering.

A spectroscopic characterization of these materials has been presented. It was verified that the optical properties of the Ni^{2+} and Co^{2+} ions in the BaLiF_3 matrix are similar to those presented by these transition-metal ions in the other octahedral-symmetry matrices. The observed infrared emission bands are centred at 1.5 μm (Ni^{2+}) and 1.6 μm (Co^{2+}). The spectroscopic characterization of both materials indicates that $\text{BaLiF}_3:\text{Ni}^{2+}$ and $\text{BaLiF}_3:\text{Co}^{2+}$ are promising laser-active media in the spectral region of 1.5 μm .

Acknowledgements

The authors acknowledge the support given by Fundação de Amparo a Pesquisa do Estado de São

Paulo – FAPESP (Research Contract No. 90/3712–8) and TWAS (Research Contract No. 140RG/PHYS/LA).

References

- [1] D. Vivien, Mater. Res. Soc. Symp. Proc. 329 (1994) 215.
- [2] S.L. Baldochi and J.Y. Gesland, Mater. Res. Bull. 27 (1992) 891.
- [3] S.L. Baldochi, V.L. Mazzocchi, C.B.R. Parente and S.P. Morato, Mater. Res. Bull. 29 (1994) 1321.
- [4] R. Leckebusch, A. Neuhaus and K. Recker, J. Crystal Growth 16 (1972) 10.
- [5] J. Granec, L. Lozano, in: Inorganic Solid Fluorides: Chemistry and Physics, Ed. P. Hagenmuller (Academic Press, New York, 1985) ch. 2.
- [6] A.M.E. Santo, S.L. Baldochi and S.P. Morato, Pesquisa e Desenvolvimento Tecnológico 19 (1995) 28.
- [7] R.A. Laudise, The growth of single crystals (Prentice–Hall, Englewood Cliffs, NJ, 1970) p. 57.
- [8] R. Lamprecht, D. Schwabe, A. Charmann and E. Schultheiss, J. Crystal Growth 65 (1993) 143.
- [9] E. Martins, N.D. Vieira, Jr., S.L. Baldochi, S.P. Morato and J.Y. Gesland, J. Luminescence 62 (1994) 281.
- [10] E. Martins, Doctor Thesis (University of São Paulo – IPEN 1994).
- [11] M. Duarte, E. Martins, S.L. Baldochi, N.D. Vieira, Jr. and M.M.F. Vieira. Anais VI Simpósio Estadual de Lasers e Aplicações. São Carlos, SP, Brazil (1994) p. 96.